



ORIGINAL ARTICLE

Enhancement of dye-sensitized solar cell efficiency through co-sensitization of thiophene-based organic compounds and metal-based N-719



Ismail Althagafi ^a, Nashwa El-Metwaly ^{a,b,*}

^a Department of Chemistry, College of Applied Sciences, Umm Al-Qura University, 21955 Makkah, Saudi Arabia

^b Chemistry Department, Faculty of Science, Mansoura University, 35516 Mansoura, Egypt

Received 26 December 2020; accepted 9 February 2021

Available online 20 February 2021

KEYWORDS

Thiophene;
Photoconversion efficiency;
Co-sensitization;
DFT

Abstract Synthesis of five novel thiophene-based metal-free organic dyes, named **IS1-5**, to study their photophysical, electrochemical properties and photovoltaic performance as sensitizers and co-sensitizers for DSSCs. Dyes **IS-5** are cyanoacetanilide derivatives, which are distinguished by their small size, the simple preparation method, and the presence of multiple anchoring species (C=O and CN) within their molecular structure. From their UV/Vis. spectra, **IS-4** and **IS-5** displayed the highest molar extinction coefficient with a bathochromic-shift to the intramolecular charge transfer band. In addition, to recognize the potential of HOMO level and the potential of LUMO level among all **IS1-5** dyes, the cyclic voltammetry technique must be used. Their characteristics assert that all dyes possess the qualifications essential to be used as a sensitizer for dye-sensitized solar cells (DSSCs). Interestingly, over co-sensitization, all dyes showed better photovoltage values (V_{OC}) than the standard dye N-719. Among Dyes **IS1-5**, co-sensitizer **IS-5** showed the highest photoconversion efficiency (η) of (8.09%) compared to the standard dye N-719 (7.61%). Moreover, electrochemical impedance spectroscopy (EIS) asserts the impact of this dye on improving charge transfer in TiO_2 . Finally, density functional theory (DFT) has been studied for dyes **IS1-5** using Gaussian09 software and the outcomes comfortably agree with experimental results.

© 2021 The Author(s). Published by Elsevier B.V. on behalf of King Saud University. This is an open access article under the CC BY-NC-ND license (<http://creativecommons.org/licenses/by-nc-nd/4.0/>).

1. Introduction

Environmental changes caused by gases resulting from burning fuels have increased interest in alternative and sustainable energy sources, which will be of interest sooner rather than the latter to achieve economic development worldwide (Abbasi et al., 1991). Proceeding from this view, the use of solar radiation by dye-sensitized solar cells (DSSCs) to produce electricity is being the introductory solution for meeting energy

* Corresponding author at: Department of Chemistry, College of Applied Sciences, Umm Al-Qura University, 21955 Makkah, Saudi Arabia.

E-mail address: nmmohamed@uqu.edu.sa (N. El-Metwaly).

Peer review under responsibility of King Saud University.



Production and hosting by Elsevier

demands (Grätzel, 2001; Wu et al., 2015). In DSSCs, the dye molecule is necessary to absorb solar energy and inject electrons into the semiconductor's conduction band. The most promising dye sensitizers are ruthenium (Ru) complexes such as N3, N-719, and black dyes (Nazeeruddin et al., 1993; Chen et al., 1996; Tang et al., 2015). Organic sensitizer of alkoxy-silyl-anchoring moiety has so far registered powerful conversion efficiencies (14.3%) (Kakiage et al., 2015). However, there are some disadvantages of using metal-based dye-sensitized solar such as many synthesis procedures, difficulty in purification and expensive materials used. As a result, several investigators have studied metal-free dyes because of their low-cost preparation, high molar extinction, the versatility of structural designs, and tunable optical and electrochemical properties (Hagfeldt et al., 2010; Wang et al., 2017). Abundant aromatic heterocyclic dyes have been used as an effective sensitizer when used in DSSCs, such as carbazole, indole, phenoxazine, phenothiazine, and coumarin (Mishra et al., 2009; Zhang et al., 2020; Nesheli et al., 2020). In addition, BODIPY and porphyrins have been used as an efficient sensitizer for DSSC to tune their optoelectronic properties (Shah et al., 2020; He et al., 2017; Islam et al., 2018; Zou et al., 2020; Lu et al., 2019; Kurumisawa et al., 2019; Mathew et al., 2014; Zeng et al., 2020).

To gain the merits of both metal-free and metal-based dyes, the co-sensitization technique involving the mixing of various types of dyes in the same manufactured cell has been used as

a promising method for enhancing the cell's photovoltaic efficiency as the dye's light-harvesting ability increases (Sharma et al., 2014; Elmorsy et al., 2020; Lee et al., 2018; Younas and Harrabi, 2020). Hence, our research project focused on the synthesis of small metal-free dyes **IS1-5** as sensitizers and co-sensitizers with the standard N-719 Ru (II) complex for DSSC applications. The newly **IS1-5** dyes possess a thiophene moiety, which has been identified as potential entities because it has good tunable spectroscopic and electrochemical characteristics (Sharmoukh et al., 2020; Giri et al., 2020). Also, dyes **IS-5** are cyanoacetanilide derivatives, which are distinguished by their small size, the simple preparation method, and the presence of multiple anchoring species (C=O and CN) within their molecular structure. Using multiple anchoring moieties within the molecular structure enhances the photovoltaic performance of the fabricated dye (Ambrosio et al., 2012; Beni et al., 2015). The chemical structure of the fabricated dyes **IS1-5** and N-719 is depicted in Fig. 1. The synthesized pathways have been displayed according to Scheme 1. All dyes **IS1-5** were characterized by ^1H NMR, ^{13}C NMR, FTIR, and mass spectroscopy. Their optical studies were investigated using UV-Vis absorption, the molecular orbital energies were calculated from cyclic voltammetric (CV) studies, and density functional theory studies (DFT) using gaussian09 software. Finally, the fabrication of novel dyes **IS1-5** as sensitizers and co-sensitizers along with N-719 (Fig. 1) for studying their photovoltaic performance as DSSCs.

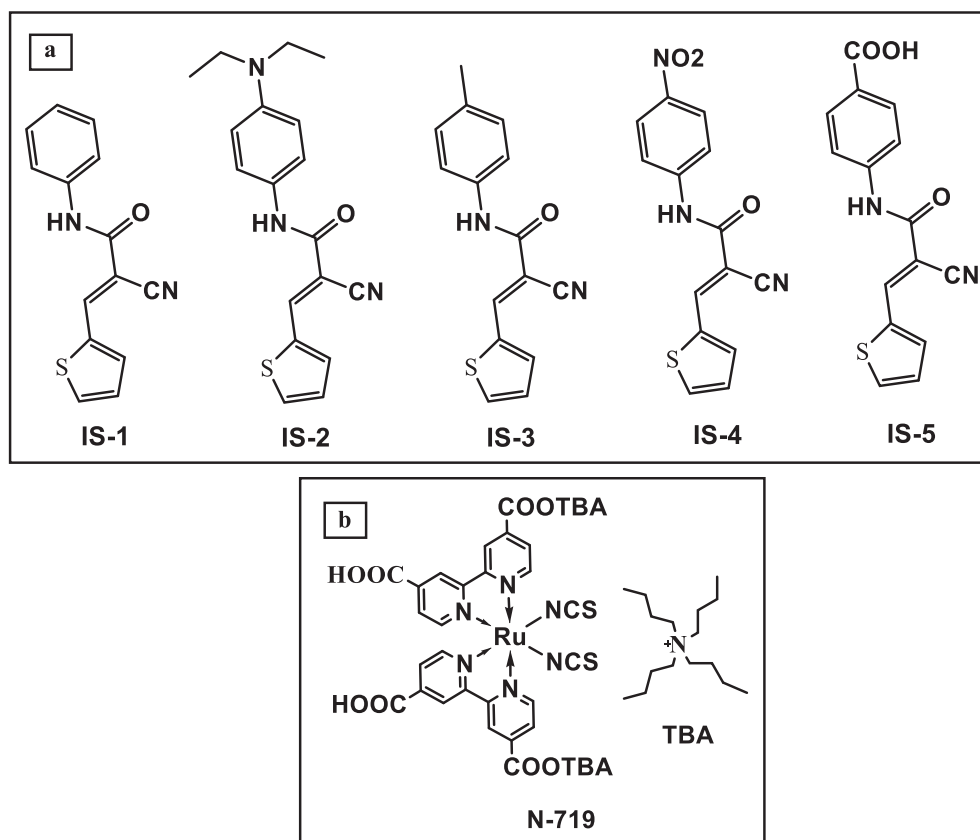
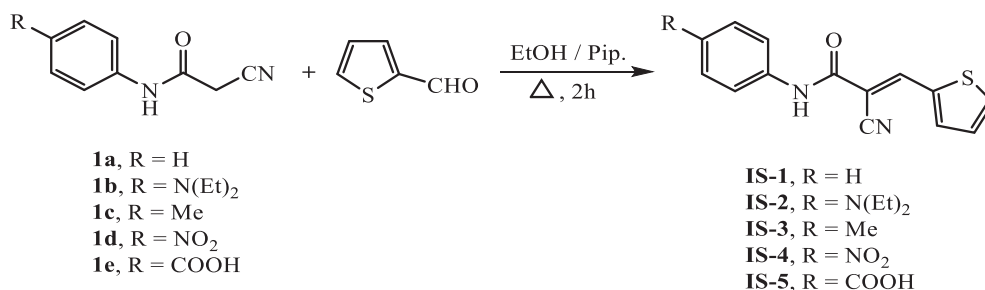


Fig. 1 Molecular structure of dyes **IS1-5** (a) and **N-719** (b).



Scheme 1 Synthetic pathway of cyanoacetanilides **IS1-5**.

2. Experimental

2.1. Synthesis and characterization

All organic solvents and reagents were acquired from TCI America and Sigma-Aldrich. The recorded melting points (°C) were measured using Gallenkamp apparatus and are uncorrected. Spectroscopic analysis such as IR and NMR spectra were detected using Thermo Scientific Nicolet iS10 FTIR spectrometer and JEOL's NMR spectrometer in DMSO *d*₆ (500 MHz for ¹H NMR and 125 MHz for ¹³C NMR), respectively. The high-performance double beam spectrophotometer (T80 series) has been used for measuring UV-Visible spectrophotometer. Elemental analyses (C, H, and N) were estimated on Perkin Elmer 2400 analyzer. Fabrication of DSSC devices and measuring photovoltaic parameters have been performed at Damietta University (Egypt). Moreover, cyclic voltammetry measurements, impedance spectroscopy techniques, solar cell fabrication devices, and solar cell characterization can be found in detail in the [supplementary file](#).

2.1.1. Synthesis of intermediates 1a-e

Intermediates **1a-e** has been investigated before, as per a known protocol ([Elmorsy et al., 2020](#)).

2.1.2. General synthesis of *N*-aryl-2-cyano-3-(thiophen-2-yl)acrylamide sensitizers **IS1-5**

To a solution of each cyanoacetanilide derivative **1a-e** (4 mmol) in 25 mL ethanol, 2-formylthiophene (0.45 mL, 4 mmol) and piperidine (0.1 mL) were added. The reaction contents were refluxed for 2 h followed by cooling to 25 °C. The precipitate that produced was collected and dried to furnish the targeted thiophene-based co-sensitizers **IS1-5**.

2.1.2.1. 2-Cyano-*N*-phenyl-3-(thiophen-2-yl)acrylamide (IS-1). Red solid (83%), m.p. = 177–179 °C. IR (ν_{max} , cm⁻¹): 3352 (—NH stretch), 2212 (—CN stretch), 1678 (—CO stretch). ¹H NMR (δ , ppm): 7.12 (t, *J* = 7.25 Hz, 1H), 7.33–7.37 (m, 3H), 7.65 (d, *J* = 7.50 Hz, 2H), 7.93 (d, *J* = 3.50 Hz, thiophene-H), 8.13 (d, *J* = 5.00 Hz, thiophene-H), 8.51 (s, 1H, C=CH), 10.28 ppm (s, 1H, NH). ¹³C NMR (δ , ppm): 102.59, 116.48, 120.59 (2C), 124.26, 128.68, 128.73 (2C), 135.34, 135.70, 138.10, 138.29, 143.88, 160.34 ppm. Mass analysis (*m/z*, %): 254 (34.23), 246 (66.11), 228 (52.46), 193 (36.01), 188 (42.15), 176 (37.56), 154 (70.20), 134 (67.00), 128 (100.00), 95 (77.30), 89 (52.89). Anal. calcd for C₁₄H₁₀N₂OS (254.05): C,

66.12; H, 3.96; N, 11.02%. Found: C, 66.02; H, 3.98; N, 11.09%.

2.1.2.2. 2-Cyano-*N*-(4-(diethylamino)phenyl)-3-(thiophen-2-yl)acrylamide (IS-2). Violet solid (65%), m.p. = 181–183 °C. IR (ν_{max} , cm⁻¹): 3419 (—NH stretch), 2212 (—CN stretch), 1663 (—CO stretch). ¹H NMR (δ , ppm): 1.06 (t, *J* = 7.00 Hz, 6H), 3.30 (q, *J* = 7.00 Hz, 6H), 6.63 (d, *J* = 9.00 Hz, 2H), 7.32 (dd, *J* = 4.00, 4.00 Hz, thiophene-H), 7.41 (d, *J* = 9.00 Hz, 2H), 7.90 (d, *J* = 4.00 Hz, thiophene-H), 8.10 (d, *J* = 4.00 Hz, thiophene-H), 8.44 (s, 1H, C=CH), 9.94 (s, 1H, NH). ¹³C NMR (δ , ppm): 12.42 (2C), 43.72 (2C), 102.82, 111.50 (2C), 116.64, 122.51 (2C), 126.61, 128.59, 134.89, 135.92, 137.73, 143.17, 144.67, 159.38 ppm. Mass analysis (*m/z*, %): 325 (46.63), 316 (52.71), 305 (25.64), 271 (100.00), 265 (51.50), 257 (53.33), 228 (55.36), 208 (37.56), 152 (41.40), 107 (25.35), 78 (39.48). Anal. calcd for C₁₈H₁₉N₃OS (325): C, 65.43; H, 4.89; N, 11.91%. Found: C, 66.51; H, 5.85; N, 11.85%.

2.1.2.3. 2-Cyano-3-(thiophen-2-yl)-*N*-(*p*-tolyl)acrylamide (IS-3). Red solid (88%), m.p. = 191–192 °C. IR (ν_{max} , cm⁻¹): 3349 (—NH stretch), 2213 (—CN stretch), 1674 (—CO stretch). ¹H NMR (δ , ppm): 2.26 (s, 3H), 7.14 (d, *J* = 8.00 Hz, 2H), 7.33 (dd, *J* = 4.50, 4.00 Hz, thiophene-H), 7.53 (d, *J* = 8.00 Hz, 2H), 7.91 (d, *J* = 3.00 Hz, thiophene-H), 8.12 (d, *J* = 5.00 Hz, thiophene-H), 8.49 (s, 1H, C=CH), 10.19 ppm (s, 1H, NH). ¹³C NMR (δ , ppm): 20.55, 102.69, 116.38, 120.70 (2C), 128.71, 129.17 (2C), 133.41, 135.26, 135.78, 135.84, 138.05, 143.75, 160.18 ppm. Mass analysis (*m/z*, %): 268 (20.38), 241 (15.33), 202 (21.80), 175 (24.66), 133.63 (30.82), 82 (56.41), 55.22 (100.00). Anal. calcd for C₁₅H₁₂N₂OS (268.07): C, 67.16; H, 4.11; N, 10.95%. Found: C, 67.35; H, 3.98; N, 11.08%.

2.1.2.4. 2-Cyano-*N*-(4-nitrophenyl)-3-(thiophen-2-yl)acrylamide (IS-4). Black solid (70%), m.p. = 203–205 °C. IR (ν_{max} , cm⁻¹): 3323 (—NH stretch), 2218 (—CN stretch), 1689 (—CO stretch). ¹H NMR (δ , ppm): 7.36 (dd, *J* = 5.00, 4.00 Hz, thiophene-H), 7.93 (d, *J* = 8.50 Hz, 2H), 7.96 (d, *J* = 3.00 Hz, thiophene-H), 8.18 (d, *J* = 4.50 Hz, thiophene-H), 8.26 (d, *J* = 9.00 Hz, 2H) 8.58 (s, 1H, C=CH), 10.75 ppm (s, 1H, NH). ¹³C NMR (δ , ppm): 102.02, 116.24, 120.18 (2C), 124.85 (2C), 128.86, 135.63, 136.10, 138.71, 142.85, 144.64, 144.88, 161.19 ppm. Mass analysis (*m/z*, %): 300 (60.40), 292 (56.27), 279 (42.65), 246 (53.08), 231 (100.00), 185 (90.90), 176 (63.45), 163 (66.46), 157 (82.42),

145 (41.32), 90 (52.73), 57 (56.86). Anal. calcd for $C_{14}H_9N_3O_3S$ (299.04): C, 56.18; H, 3.03; N, 14.04%. Found: C, 56.28; H, 3.00; N, 14.11%.

2.1.2.5. 4-(2-Cyano-3-(thiophen-2-yl)acrylamido)benzoic acid (IS-5). Black solid (62%), m.p. = 239–241 °C. IR (ν_{max} , cm^{-1}): 3332 (—NH stretch), 2218 (—CN stretch), 1677 (—CO stretch). 1H NMR (δ , ppm): 7.35 (dd, J = 5.00, 3.50 Hz, thiophene-H), 7.78 (d, J = 9.00 Hz, 2H), 7.93 (d, J = 9.00 Hz, 2H), 7.94 (d, J = 3.00 Hz, thiophene-H), 8.15 (d, J = 5.00 Hz, thiophene-H), 8.55 (s, 1H, =CH), 10.58 (s, 1H, NH), 12.86 (s, 1H, COOH). ^{13}C NMR (δ , ppm): 102.38, 116.37, 119.75 (2C), 126.14, 128.77, 130.29 (2C), 135.71 (2C), 138.39, 142.41, 144.33, 160.80, 166.89 ppm. Mass analysis (m/z , %): 298 (10.77), 292 (80.58), 270 (50.43), 242 (18.75), 173 (8.01), 82 (41.13), 77 (64.76), 54 (100.00). Anal. calcd. for $C_{15}H_{10}N_2O_3S$ (298.04): C, 60.38; H, 3.37; N, 9.96%. Found: C, 60.23; H, 2.29; N, 10.08%.

3. Result and discussion

3.1. Structural designing and synthesis

Cyanoacetanilide derivatives **1a-e** have been synthesized through refluxing 1-cyanoacetyl-3,5-dimethylpyrazole with *N*, *N*-diethyl-*p*-phenylenediamine, aniline, 4-toluidine, 4-aminobenzoic acid, and 4-nitroaniline, respectively, as reported in the literature. Then, **IS1-5** precursors were achieved by following Knoevenagel reaction conditions between different **1a-e** cyanoacetanilides and 2-formyl thiophene in presence of piperidine as a catalyst in a boiling solution of EtOH (Scheme 1).

3.2. UV-visible studies

Fig. 2 showed the UV-visible absorbance spectra for **IS1-5** in chloroform medium (2×10^{-5} M) and their related spectral data are stated in Table 1.

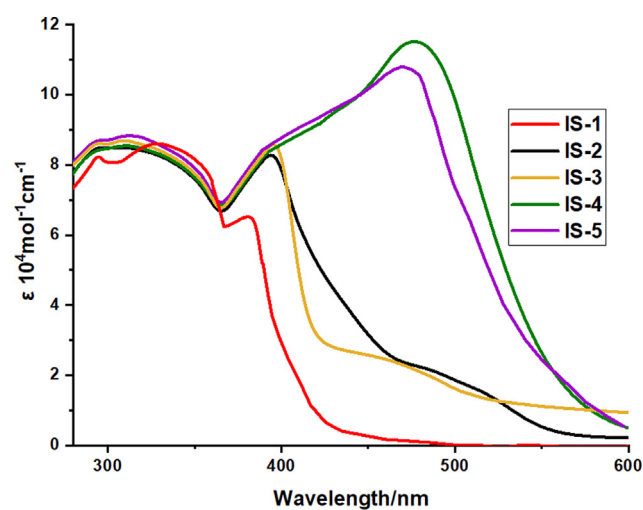


Fig. 2 UV-Vis absorption of **IS1-5** in $CHCl_3$ (2×10^{-5} M).

All dyes **IS1-5** showed two obvious absorption bands. The first band related to $\pi \rightarrow \pi^*$ appeared in the region from 330 to 400 nm while a second band from 400 to 570 nm reflected the internal charge transfer from the donor to the acceptor.

Further, Dyes **IS-4** and **IS-5** containing $-NO_2$ and $-COOH$ anchoring species, respectively showed broadening in their spectra with a red-shift in their lowest energy band due to the extension of the conjugation within molecular frames. Moreover, band energy gaps (E_{0-0}) were measured from their UV/Vis. spectra showed an agreement with theoretical values calculated from DFT studies (Al-Eid et al., 2014). From the results, dye **IS-4** exhibited the least band gap value that can be attributed to

the nitro group's good withdrawal capacity.

Moreover, the absorption spectra of products **IS1-5** adsorbed onto TiO_2 film are shown in Fig. 3. The spectra were broadened due to the interaction between sensitizers and TiO_2 (Li et al., 2006). The broadening in the spectra indicated that most sensitizers were adsorbed on the TiO_2 surface. Besides, dye **IS-5** bearing carboxyl group $-COOH$ as an anchoring moiety is found to be even more adsorbed on TiO_2 than other compounds **IS1-4**, providing a good indication of this dye's better photovoltaic efficiency.

3.3. Computational studies

Optimization of the ground state geometries and frontier molecular orbitals (FMOs) of dyes **IS1-5** were performed using density functional theory (DFT) by Gaussian09 software at B3LYP/6-311G (d, p) level (Frisch et al., 2017). The calculated E_{0-0} and orbital energies agreed well with cyclic voltammetry results. Fig. 4 depicts the simulated FMOs of dyes **IS1-5**.

The outcomes showed variations in electron distributions in their HOMO-Level, which may be attributed to their structural nature. For dye **IS-1**, there is symmetry in the electron distribution for the GSOP/HOMO and ESOP/LUMO which may be attributed to the absence of strong donating/accepting moiety. This observation indicates a poor charge transfer of the former dye. For Dyes **IS-2** and **IS-3**, which contain *N*, *N*-diethyl, and methyl moiety, respectively, the electron distribution is concentrated on the phenyl ring for their HOMO levels, while in their LUMO levels, the electron is concentrated in the thiophene moiety. In contrast, Dyes **IS-4** and **IS-5** show opposite behavior, in their HOMO levels, the electron distribution mainly concentrated on the thiophene ring, while in their LUMO levels, the electron concentrated on the phenyl ring due to the presence of strong accepting moieties ability ($-NO_2$ and $-COOH$) beside the benzene ring. From the aforementioned, Dyes **IS2-5** are expected to show good charge transfer from The HOMO to LUMO, which could be translated to better performance.

3.4. Cyclic voltammetry experiments (CV)

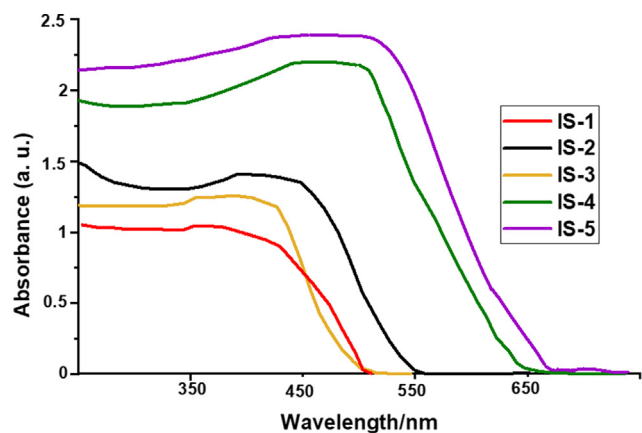
Excited state oxidation potentials (ESOPs) and ground state oxidation potentials (GSOPs) of all dyes were measured by cyclic voltammetry techniques (Fig. 5).

First of all, GSOPs were calculated from oxidation onset of cyclic voltammogram as shown in equation 1:

$$GSOP = -[\text{Oxidation onset} + 4.7] \text{ eV} \quad (1)$$

Table 1 Optical properties of IS1-5.

Dyes	λ (nm)	ϵ ($10^4 \text{ M}^{-1}\text{cm}^{-1}$)	E_{0-0} Experimental (λ_{onset})	E_{0-0} (theoretical)
IS-1	336, 381	8.52, 6.51	2.96	2.95
IS-2	393, 390	5.23, 8.47	2.58	2.55
IS-3	396, 394	8.56, 8.25	2.74	2.81
IS-4	396, 477	8.71, 11.51	2.49	2.43
IS-5	396, 471	8.41, 10.74	2.53	2.47

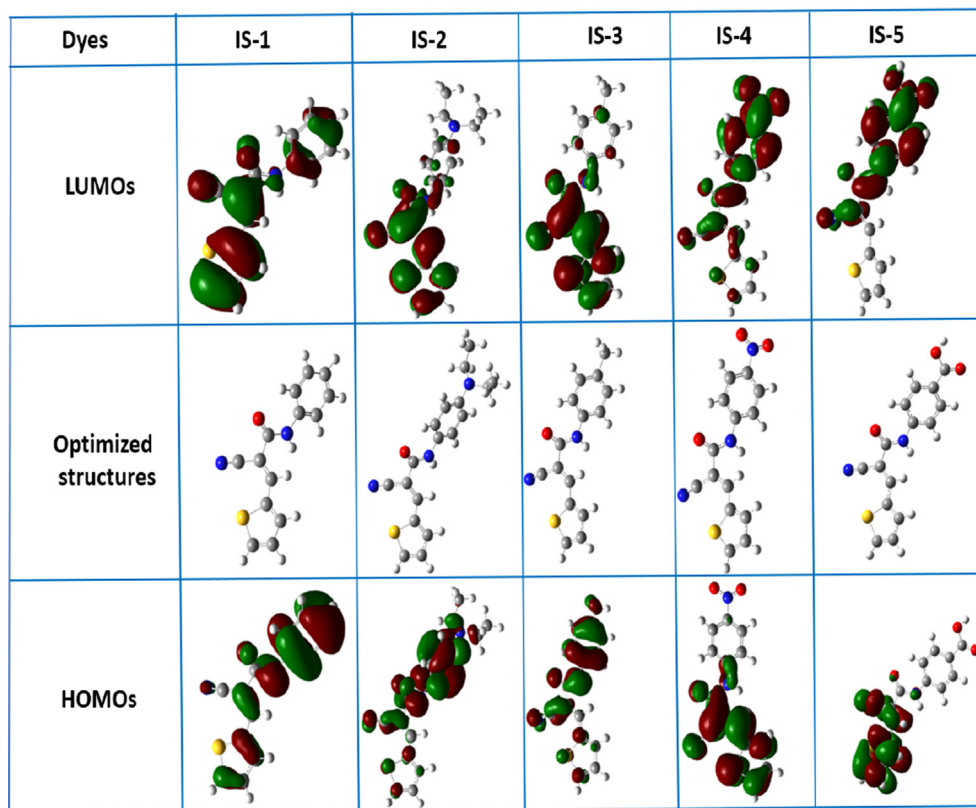
**Fig. 3** UV-Vis absorption of IS1-5 anchored onto nonporous TiO_2 .

Then, ESOPs was derived from the values of E_{0-0} and GSOP as shown in equation 2:

$$\text{ESOP} = [\text{GSOP} - E_{0-0}] \text{ eV} \quad (2)$$

An ideal dye should include some thermodynamic criteria for being used as DSSC; The GSOP levels should be below the redox potential of the electrolyte (-5.2 eV) and the ESOP levels should be above the conduction band of nanocrystalline TiO_2 layer (-4.2 eV) (Qu and Meyer, 2001; Oskam et al., 2001) as shown in Fig. 6.

From the results in Table 2, the estimated values of GSOP for IS1-5 were found to be; IS-1 (-6.02 eV), IS-2 (-5.61 eV), IS-3 (-5.59 eV) and IS-4 (-5.46 eV) and IS-5 (-5.44), below the redox potential of the electrolyte for better dye regeneration. Also, the measured ESOPs were found to be; IS-1 (-3.06 eV), IS-2 (-2.98 eV), IS-3 (-3.01 eV), IS-4 (-2.97 eV) and IS-5 (-2.91 eV), above the conduction band potential of the TiO_2 for better electron injection.

**Fig. 4** Optimized structures and simulated FMOs of IS1-5.

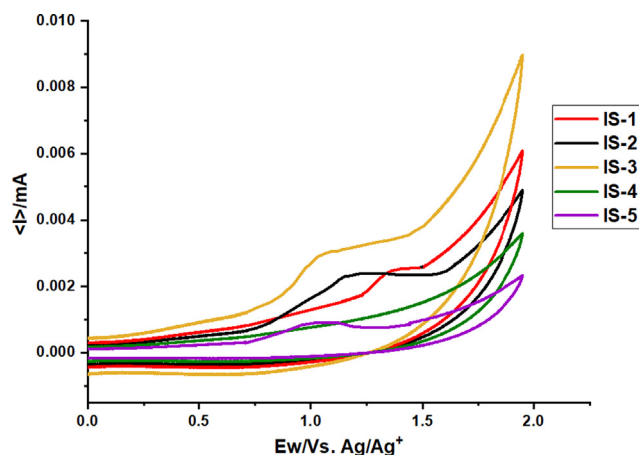


Fig. 5 Cyclic voltammery traces for IS1-5.

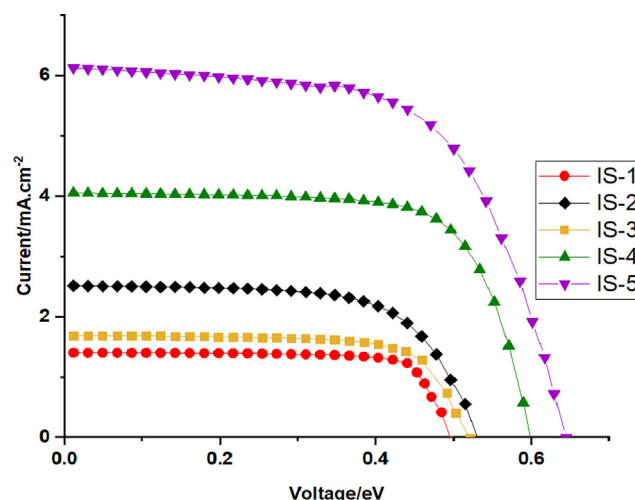


Fig. 7 J - V curves of the fabricated devices IS1-5.

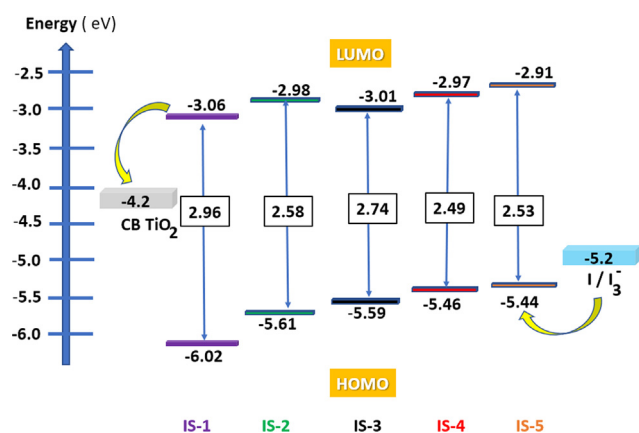


Fig. 6 Energy level diagram of IS1-5 based on the experimental values.

Further, IS-5 possess the highest negative free energy of (1.29 eV), which represents a good indication of the best injection of electron to TiO₂ band and so IS-5 is expected to give a good photovoltaic performance compared to other dyes IS1-4.

3.5. Photovoltaic parameters measurements

DSSCs were fabricated using five novel metal free dyes IS1-5 alone and co-sensitized with N-719. The fabrication procedure and instruments were discussed briefly in the supplementary file. Chenodeoxycholic acid “CDCA” was added into the dye

solution as a co-adsorbent to diminish the dye aggregation and suppress recombination reactions, which ultimately leads to enhanced V_{OC} values as well as total efficiency of the fabricated devices (Neale et al., 2005; Ito et al., 2008). Fig. 7 displays the J - V curves of the fabricated cells IS1-5 alone. Their corresponding photovoltaic parameters are presented in Table 3. Under standard global AM 1.5 solar conditions, the cells employing IS1-5 sensitizers yielded PCE of 0.49, 0.89, 0.64, 1.69 and 2.72%, respectively. The IS-5 sensitized cell showed better photovoltaic parameters values: $J_{sc} = 6.15$ mA/cm², $V_{oc} = 0.646$ V and $FF = 68.30$ compared to other dyes IS1-4. Increasing J_{sc} value of IS-5 can be attributed to an efficient anchoring moiety (–COOH). The better anchoring moiety (–COOH) led to better charge transfer from The HOMO to the LUMO which, allowing electron injection to the TiO₂ edge conduction band (Koops et al., 2009). On the other hand, the low performances of dyes IS1-3 can be related to the absence of good anchoring moieties as observed from the low adsorption of these dyes to TiO₂ nanoparticles (Fig. 3) (Cheema et al., 2009). Besides this reason, there is symmetry in electron distribution of the HOMO/LUMO of dye IS-1 leading to poor charge transfer and hence the lowest performance (0.49%) (Montiel et al., 2019).

In order to study the effect of co-sensitization of IS1-5 along with the standard Ru based N-719 dye, the devices were fabricated using 0.2 mM of N-719 dye and 0.2 mM of co-sensitizer IS1-5. Fig. 8 displays the J - V curves of the photovoltaic devices co-sensitized with dyes IS-5. Their correspond-

Table 2 Electrochemical properties of IS1-5.

Structure	Experimental (eV)			Theoretical (eV)	
	E_{ox} (V)	GSOP	ESOP	GSOP	ESOP
IS-1	1.32	–6.02	–3.06	–6.12	–3.17
IS-2	0.91	–5.61	–2.98	–5.52	–3.09
IS-3	0.89	–5.59	–3.01	–5.70	–3.15
IS-4	0.76	–5.46	–2.97	–5.53	–3.06
IS-5	0.74	–5.44	–2.91	–5.72	–2.91

4. Conclusions

Five organic compounds **IS1-5** have been engineered as sensitizers for DSSCs. Further, the performance of a DSSC using co-sensitization was improved in this study. **IS1-5** co-sensitizers were used with N-719, a ruthenium-based dye (II). Dyes (**IS1-5**) showed better V_{OC} values over co-sensitization with N-719 of using individual N-719. **IS-5** showed the best impact on N-719's photovoltaic efficiency with a PCE of 8.09%, J_{SC} (19.23) and V_{OC} (0.680) compared to PCE of 7.61%, J_{SC} (18.59) and V_{OC} (0.658 eV) of N-719. Dyes **IS-4** and **IS-5** containing $-\text{NO}_2$ and $-\text{COOH}$ anchoring species, respectively showed broadening in their spectra with a red-shift in their lowest energy band due to the extension of conjugation within molecular frames. Finally, in accordance with the experimental data, simulation studies based on DFT studies were used.

Declaration of Competing Interest

The authors declare that they have no known competing financial interests or personal relationships that could have appeared to influence the work reported in this paper.

Acknowledgements

The authors would like to thank Deanship of Scientific Research at Umm Al-Qura University, Saudi Arabia (project ID: 19-SCI-1-01-0001) for the financial support to this research extracted from the project.

Appendix A. Supplementary material

Supplementary data to this article can be found online at <https://doi.org/10.1016/j.arabjc.2021.103080>.

References

- Abbasi, T., Premalatha, M., Abbasi, S., 1991. The return to renewables: Will it help in global warming control. *Renew. Sustain. Energy Rev.* 15, 891–894. <https://doi.org/10.1016/j.rser.2010.09.048>.
- Al-Eid, M., Limb, S., Park, K., Fitzpatrick, B., Han, C., Kwak, K., Hong, J., Cooke, G., 2014. Facile synthesis of metal-free organic dyes featuring a thienylethynyl spacer for dye sensitized solar cells. *Dyes Pigm.* 104, 197–203. <https://doi.org/10.1016/j.dyepig.2014.01.004>.
- Ambrosio, F., Martsinovich, N., Troisi, A., 2012. Effect of the anchoring group on electron injection: theoretical study of phosphonated dyes for dye-sensitized solar cells. *J. Phys. Chem. C* 116, 2622–2629. <https://doi.org/10.1021/jp209823t>.
- Beni, A.S., Zarandi, M., Madram, A.R., Bayat, Y., Chermahini, A.N., Ghahary, R., 2015. Synthesis and characterization of organic dyes bearing new electron-withdrawing group for dye-sensitized solar cells. *Electrochim. Acta* 186, 504–511. <https://doi.org/10.1016/j.electacta.2015.10.172>.
- Cheema, H., Islam, A., Han, L., El-Shafei, A., 2009. Influence of number of benzodioxan-stilbazole-based ancillary ligands on dye packing, photovoltage and photocurrent in dye-sensitized solar cells. *ACS Appl. Mater. Interfaces* 6, 11617–11624. <https://doi.org/10.1021/am502400b>.
- Chen, F., Mehta, P.G., Takiff, L., McCullough, R.D., 1996. Improved electroluminescence performance of poly (3-alkylthiophenes) having a high head-to-tail (HT) ratio. *J. Mater. Chem.* 6, 1763–1766. <https://doi.org/10.1039/JM9960601763>.
- Elmorsy, M.R., Lyu, L., Su, R., Abdel-Latif, E., Badawy, S.A., El-Shafei, A., Fadda, A.A., 2020. Co-sensitization of the HD-2 complex with low-cost cyanoacetanilides for highly efficient DSSCs. *Photochem. Photobiol. Sci.* 19, 281–288. <https://doi.org/10.1039/C9PP00381A>.
- Elmorsy, M.R., Abdel-Latif, E., Badawy, S.A., Fadda, A.A., 2020. Molecular geometry, synthesis and photovoltaic performance studies over 2-cyanoacetanilides as sensitizers and effective co-sensitizers for DSSCs loaded with HD-2. *J. Photochem. Photobiol. A.* 389, (15). <https://doi.org/10.1016/j.jpphotochem.2019.112239>.
- M. J. Frisch, G. W. Trucks, H. B. Schlegel, G. E. Scuseria, M. A. Robb, J. R. Cheeseman, G. Scalmani, V. Barone, B. Mennucci, G. A. Petersson, H. Nakatsuji, M. Caricato, X. Li, H. P. Hratchian, A. F. Izmaylov, J. Bloino, G. Zheng, J. L. Sonnenberg, M. Hada, M. Ehara, K. Toyota, R. Fukuda, J. Hasegawa, M. Ishida, T. Nakajima, Y. Honda, O. Kitao, H. Nakai, T. Vreven, J. A. Montgomery Jr., J. E. Peralta, F. Ogliaro, M. Bearpark, J. J. Heyd, E. Brothers, K. N. Kudin, V. N. Staroverov, R. Kobayashi, J. Normand, K. Raghavachari, A. Rendell, J. C. Burant, S. S. Iyengar, J. Tomasi, M. Cossi, J. M. Rega, J. M. Millam, M. Klene, J. E. Knox, J. B. Cross, V. Bakken, C. Adamo, J. Jaramillo, R. Gomperts, R. E. Stratmann, O. Yazyev, A. J. Austin, R. Cammi, Eur. J. Inorg. Chem. 2017, 3690–3697 www.eurjic.org 3697 © 2017 Wiley-VCH Verlag GmbH & Co. KGaA, Weinheim C. Pomelli, J. W. Ochterski, R. L. Martin, K. Morokuma, V. G. Zakrzewski, G. A. Voth, P. Salvador, J. J. Dannenberg, S. Dapprich, A. D. Daniels, Ö. Farkas, J. B. Foresman, J. V. Ortiz, J. Cioslowski, D. J. Fox, Gaussian 09, Revision A.02, Gaussian, Inc., Wallingford CT, 2009.
- Giri, D., Raut, S.K., Patra, S.K., 2020. Diketopyrrolopyrrole/perylene-diimide and thiophene based D- π -A low bandgap polymer sensitizers for application in dye sensitized solar cells. *Dyes Pigments* 174. <https://doi.org/10.1016/j.dyepig.2019.108032>.
- Grätzel, M., 2001. Photoelectrochemical cells. *Nature* 414, 338–344. <https://doi.org/10.1038/35104607>.
- Hagfeldt, A., Boschloo, G., Sun, L., Kloo, L., Pettersson, H., 2010. Dye-sensitized solar cells. *Chem. Rev.* 110, 6595–6663. <https://doi.org/10.1021/cr900356p>.
- He, H., Bosonetta, J., Wheeler, K., May, S.P., 2017. Sisters together: co-sensitization of near-infrared emission of ytterbium (III) by BODIPY and porphyrin dyes. *Chem. Commun.* 53, 10120–10123. <https://doi.org/10.1039/C7CC05437H>.
- Hua, Y., Jin, B., Wang, H., Zhu, X., Wu, W., Sing Cheung, M., Lin, Z., Wong, W., Wong, W., 2013. Bulky dendritic triarylamine-based organic dyes for efficient co-adsorbent-free dye-sensitized solar cells. *J. Power Sources* 237, 195–203. <https://doi.org/10.1016/j.jpowsour.2013.03.018>.
- Islam, A., Chowdhury, T., Qin, C., Han, L., Lee, J., Bedja, I., Akhtaruzzaman, M., Sopian, K., Mirloup, A., Leclerc, N., 2018. Panchromatic absorption of dye sensitized solar cells by co-sensitization of triple organic dyes. *Sustain. Energy Fuels* 2, 209–214. <https://doi.org/10.1039/C7SE00362>.
- Ito, S., Miura, H., Uchida, S., Takata, M., Sumioka, K., Liska, P., 2008. High-conversion efficiency organic dye-sensitized solar cells with a novel indoline dye. *Chem. Commun.*, 5194–5196 <https://doi.org/10.1039/B809093A>.
- Kakiage, K., Aoyama, Y., Yano, T., Oya, K., Fujisawab, J., Hanaya, M., 2015. Highly-efficient dye-sensitized solar cells with collaborative sensitization by silyl-anchor and carboxy-anchor dyes. *Chem. Commun.* 51, 15894–15897. <https://doi.org/10.1039/C5CC06759F>.
- Koops, S.E., O'Regan, B.C., Barnes, P.R.F., Durrant, J.R., 2009. Parameters influencing the efficiency of electron injection in dye-sensitized solar cells. *J. Am. Chem. Soc.* 131, 4808–4818. <https://doi.org/10.1021/ja8091278>.

- Kurumisawa, Y., Higashino, T., Nimura, S., Tsuji, Y., Iiyama, H., Imahori, H., 2019. Renaissance of Fused Porphyrins: Substituted Methylene-Bridged Thiophene-Fused Strategy for High-Performance Dye-Sensitized Solar Cells. *J. Am. Chem. Soc.* 141 (25), 9910–9919. <https://doi.org/10.1021/jacs.9b03302>.
- Lee, H., Kim, J., Kim, D.Y., Seo, Y., 2018. Co-sensitization of metal free organic dyes in flexible dye sensitized solar cells. *Org. Electron.* 52, 103–109. <https://doi.org/10.1016/j.orgel.2017.10.003>.
- Li, S., Jiang, K., Shaoab, K., Yang, L., 2006. Novel organic dyes for efficient dye-sensitized solar cells. *Chem. Commun.*, 2792–2794 <https://doi.org/10.1039/B603706B>.
- Lu, Y., Song, H., Li, X., Ågren, H., Liu, Q., Zhang, J., Zhang, X., Xie, Y., 2019. Multiply Wrapped Porphyrin Dyes with a Phenothiazine Donor: A High Efficiency of 11.7% Achieved through a Synergetic Coadsorption and Cosensitization Approach. *ACS Appl. Mater. Interfaces.* 11 (5), 5046–5054. <https://doi.org/10.1021/acscami.8b19077>.
- Mathew, S., Yella, A., Gao, P., Humphry-Baker, R., Curchod, B.F.E., Ashari-Astani, N., Tavernelli, I., Rothlisberger, U., Khaja Nazeeruddin, Md., Grätzel, M., 2014. Dye-sensitized solar cells with 13% efficiency achieved through the molecular engineering of porphyrin sensitizers. *Nature Chem.* 6, 242–247. <https://doi.org/10.1038/nchem.1861>.
- Mishra, A., Fischer, K.K.R., Bäuerle, P., 2009. Metal-free organic dyes for dyesensitized solar cells: from structure: property relationships to design rules. *Angew. Chem. Int. Ed.* 48, 2474–2499. <https://doi.org/10.1002/anie.200804709>.
- Montiel, T., Rojo, R., López, J., Mitnik, D., 2019. Theoretical Study of the Effect of Different π Bridges Including an Azomethine Group in Triphenylamine-Based Dye for Dye-Sensitized Solar Cells. *Molecules* 24 (21), 3897. <https://doi.org/10.3390/molecules24213897>.
- Nazeeruddin, M.K., Kay, A., Rodicio, I., Humphry-Baker, R., Mueller, E., Liska, P., Vlachopoulos, N., Graetzel, M., 1993. Conversion of light to electricity by cis-X2bis (2,2'-bipyridyl-4,4'-dicarboxylate)ruthenium(II) charge-transfer sensitizers (X = Cl, Br, I, CN-, and SCN-) in nanocrystalline titanium dioxide electrodes. *J. Am. Chem. Soc.* 115, 6382–6390. <https://doi.org/10.1021/ja00067a063>.
- Neale, N.R., Kopidakis, N., van de Lagemaat, J., Grätzel, M., Frank, A.J., 2005. Effect of a coadsorbent on the performance of dye-sensitized TiO₂ solar Cells: shielding versus band-edge movement. *J. Phys. Chem. B* 109, 23183–23189. <https://doi.org/10.1021/jp0538666>.
- Nesheli, F.G., Tajbakhsh, M., Hosseinzadeh, B., Hosseinzadeh, R., 2020. Design, Synthesis and Photophysical Analysis of New Unsymmetrical Carbazole-Based Dyes for Dye-Sensitized Solar Cells. *J. Photochem. Photobiol. A* 397 (15), 11252. <https://doi.org/10.1016/j.jphotochem.2020.11252>.
- Oskam, G., Bergeron, B., Meyer, G., Searson, P., 2001. pseudohalogen for dye-sensitized Ti photoelectrochemical cells. *J. Phys. Chem. B* 105, 6867–6873. <https://doi.org/10.1021/jp004411d>.
- Oskam, G., Bergeron, B.V., Meyer, G.J., Searson, P.C., 2001. Pseudohalogen for dye-sensitized TiO₂ photoelectrochemical cells. *J. Phys. Chem. B* 105, 6867–6873. <https://doi.org/10.1021/jp004411d>.
- Qu, P., Meyer, G.J., 2001. Proton-controlled electron injection from molecular excited states to the empty states in nanocrystalline TiO₂. *Langmuir* 17, 6720–6728. <https://doi.org/10.1021/la010939d>.
- Shah, M., Mirloup, A., Chowdhury, T., Sutter, A., Hanbazazah, A., Ahmed, A., Lee, J., Abdel-Shakour, M., Leclerc, N., Kaneko, R., Islam, A., 2020. Cross-conjugated BODIPY pigment for highly efficient dye sensitized solar cells. *Sustain. Energy Fuels* 4, 1908–1914.
- Sharma, G.D., Zervaki, G.E., Angaridis, P.A., Vatikioti, A., Gupta, K.S.V., Gayathri, T., Nagarjuna, P., Singh, S.P., Chandrasekharan, M., Banthiya, A., Bhanuprakash, K., Petrou, A., Coutsolelos, A.G., 2014. Stepwise co-sensitization as a useful tool for enhancement of power conversion efficiency of dye-sensitized solar cells: the case of an unsymmetrical porphyrin dyad and a metal-free organic dye. *Org. Electron.* 15, 1324–1337. <https://doi.org/10.1016/j.orgel.2014.03.033>.
- Sharmoukh, W., Cong, J., Ali, B.A., Allam, N.K., Kloo, L., 2020. Comparison between Benzothiadiazole–Thiophene-and Benzothiadiazole–Furan-Based D-A- π -A Dyes Applied in Dye-Sensitized Solar Cells: Experimental and Theoretical Insights. *ACS Omega* 5, 16856–16864. <https://doi.org/10.1021/acsomega.0c02060>.
- Su, R., Lyu, L., Elmorsy, M., El-Shafei, A., 2019. Novel metal-free organic dyes constructed with the D-D'A- π -A motif: Sensitization and co-sensitization study 194, 400–414. <https://doi.org/10.1016/j.solener.2019.10.061>.
- Tang, Y., Wang, Y., Li, X., Ågren, H., Zhu, W.-H., Xie, Y., 2015. Porphyrins containing triphenylamine donor and up to eight alkoxy chains for dye-sensitized solar cells: a high efficiency of 10.9%. *ACS Appl. Mater. Interfaces* 7, 27976–27985. <https://doi.org/10.1021/acscami.5b10624>.
- Wang, J.C., Hill, S.P., Dilbeck, T., Ogunsolu, O.O., Banerjee, T., Hanson, K., 2017. Multimolecular assemblies on high surface area metal oxides and their role in interfacial energy and electron transfer. *Chem. Soc. Rev.* 47, 104–148. <https://doi.org/10.1039/C7CS00565B>.
- Wu, J., Lan, Z., Lin, J., Huang, M., Huang, Y., Fan, L., Luo, G., 2015. Electrolytes in dyesensitized solar cells. *Chem. Rev.* 115, 2136–2173. <https://doi.org/10.1021/cr400675m>.
- Younas, M., Harrabi, K., 2020. Performance enhancement of dye-sensitized solar cells via co-sensitization of ruthenium (II) based N749 dye and organic sensitizer RK1. *Sol. Energy* 203, 260–266. <https://doi.org/10.1016/j.solener.2020.04.051>.
- Zeng, K., Chen, Y., Zhu, W.H., Tian, H., Xie, Y., 2020. Efficient Solar Cells Based on Concerted Companion Dyes Containing Two Complementary Components: An Alternative Approach for Cosensitization. *J Am Chem Soc.* 142 (11), 5154–5161. <https://doi.org/10.1021/jacs.9b12675>.
- Zhang, W., Dai, X., Liao, X., Zang, X., Zhang, H., Yin, X., Yu, C., Ke, C., Hong, Y., 2020. Phenothiazine (or phenoxazine) based (D- π -A)-L2-(A- π -D- π -A)₂-type organic dyes with five anchors for efficient dye-sensitized solar cells. *Sol. Energy* 212, 220–230. <https://doi.org/10.1016/j.solener.2020.11.008>.
- Zou, J., Yan, Q., Li, C., Lu, Y., Tong, Z., Xie, Y., 2020. Light-Absorbing Pyridine Derivative as a New Electrolyte Additive for Developing Efficient Porphyrin Dye-Sensitized Solar Cell. *ACS Appl. Mater. Interfaces.* 12 (51), 57017–57024. <https://doi.org/10.1021/acscami.0c16427>.